

The Region of Validity of Homogeneous Nucleation Theory

A. Strumia^(a), N. Tetradis^(b) and C. Wetterich^(c)

(a) *Dipartimento di Fisica, Università di Pisa and INFN, sezione di Pisa, I-56127 Pisa, Italy*

(b) *Scuola Normale Superiore, Piazza dei Cavalieri 7, I-56126 Pisa, Italy*

(c) *Institut für Theoretische Physik, Universität Heidelberg, Philosophenweg 16, D-69120 Heidelberg, Germany*

Abstract

We examine the region of validity of Langer's picture of homogeneous nucleation. Our approach is based on a coarse-grained free energy that incorporates the effect of fluctuations with momenta above a scale k . The nucleation rate $I = A_k \exp(-S_k)$ is exponentially suppressed by the action S_k of the saddle-point configuration that dominates tunnelling. The factor A_k includes a fluctuation determinant around this saddle point. Both S_k and A_k depend on the choice of k , but, for $1/k$ close to the characteristic length scale of the saddle point, this dependence cancels in the expression for the nucleation rate. For very weak first-order phase transitions or in the vicinity of the spinodal decomposition line, the pre-exponential factor A_k compensates the exponential suppression $\exp(-S_k)$. In these regions the standard nucleation picture breaks down. We give an approximate expression for A_k in terms of the saddle-point profile, which can be used for quantitative estimates and practical tests of the validity of homogeneous nucleation theory.

1. Introduction: The theory of first-order phase transitions is a subject of much interest to statistical and particle physicists (for a review see ref. [1] and references therein). Our present understanding of these phenomena is based on the work of Langer on homogeneous nucleation theory [2]. His formalism has been applied to relativistic field theory by Coleman and Callan [3] and extended to thermal equilibrium by Affleck and Linde [4]. The basic quantity in this approach is the nucleation rate $I = A \exp(-S)$, which gives the probability per unit time and volume to nucleate a region of the stable phase (the true vacuum) within the metastable phase (the false vacuum). For a strong enough first-order transition the rate is exponentially suppressed by the free energy of the critical bubble, which is a static configuration (usually assumed to be spherically symmetric) within the metastable phase, whose interior consists of the stable phase. Bubbles larger than the critical one expand rapidly, thus converting the metastable phase into the stable one. Deformations of the critical bubble in the thermal bath generate a fluctuation

determinant around the critical-bubble configuration which is contained in A . Another dynamical prefactor determines the fast growth rate of bubbles larger than the critical one [2, 5]. We concentrate here on the calculation of the static prefactor.

Up to the dynamical prefactor, the bubble-nucleation rate is $I \sim \exp\{-\Gamma[\phi_b(r)] - \Gamma[\phi_f]\}$, with Γ the free energy, evaluated either at the false vacuum where Γ has a local minimum for a constant field ϕ_f , or for the inhomogeneous field configuration $\phi_b(r)$ which interpolates between the two vacua and is a saddle point of Γ . This configuration is usually identified with the critical bubble. The problem of computing $\Gamma[\phi_b]$ may be divided into three steps: In the first step, one only includes fluctuations with momenta larger than a scale k which is of the order of the typical gradients of $\phi_b(r)$. For this step one can consider approximately constant fields ϕ and use a derivative expansion for the resulting coarse-grained free energy $\Gamma_k[\phi]$. The second step searches for the configuration $\phi_b(r)$ which is a saddle point of Γ_k . Finally, the remaining fluctuations with mo-

menta smaller than k are evaluated in a saddle-point approximation around $\phi_b(r)$. This procedure of coarse graining systematically avoids problems with double-counting the effect of fluctuations, the convexity of the effective potential that determines part of $\Gamma[\phi_b]$, or the ultraviolet regularization of the fluctuation determinants in A [6]. As a test of the validity of the approach, the result for the rate I must be independent of the coarse-graining scale k , as the latter should be considered only as a technical device. Langer's approach corresponds to a one-loop approximation around the dominant saddle point for fluctuations with momenta smaller than k , whereas the coarse-grained free energy Γ_k is often chosen phenomenologically.

2. The method: We employ the formalism of the effective average action Γ_k [7], which can be identified with the free energy at a given coarse-graining scale k . In the limit $k \rightarrow 0$, Γ_k becomes equal to the effective action. We consider a statistical system with one space-dependent degree of freedom described by a real scalar field $\phi(x)$. For example, $\phi(x)$ may correspond to the density for the gas/liquid transition, or to a difference in concentrations for chemical phase transitions, or to magnetization for the ferromagnetic transition. Our discussion also applies to a quantum field theory in thermal equilibrium for scales k below the temperature T . Then an effective three-dimensional description [8] applies and we assume that Γ_{k_0} has been computed (for example perturbatively) for $k_0 = T$.

We approximate Γ_k by a standard kinetic term and a general potential U_k . This is expected to be a good approximation, because the size of the higher-derivative terms is related to the anomalous dimension of the field, which is small for this model ($\eta \simeq 0.035$). At a short-distance scale $k_0^{-1} = T^{-1}$, the long-range collective fluctuations are not yet important and we assume a potential

$$U_{k_0}(\phi) = \frac{1}{2}m_{k_0}^2\phi^2 + \frac{1}{6}\gamma_{k_0}\phi^3 + \frac{1}{8}\lambda_{k_0}\phi^4. \quad (1)$$

The parameters $m_{k_0}^2$, γ_{k_0} and λ_{k_0} depend on T . This potential has the typical form relevant for first-order phase transitions in four-dimensional field theories at high temperature. Through a shift $\phi \rightarrow \phi + c$ the cubic term can be eliminated in favour of a term linear in ϕ [15, 6]. The potential (1) therefore describes statistical systems of the Ising universality class in the presence of an external magnetic field. For a Hamiltonian

$$H = \int d^3x \left\{ \frac{\hat{\lambda}}{8} (\chi^2 - 1)^2 - B\chi + \frac{\zeta}{2} \partial_i \chi \partial^i \chi \right\}, \quad (2)$$

the parameters are $m_{k_0}^2 = \hat{\lambda}(3y^2 - 1)/2\zeta$, $\gamma_{k_0} = 3\hat{\lambda}T^{1/2}y/\zeta^{3/2}$, $\lambda_{k_0} = \hat{\lambda}T/\zeta^2$, with y given by $y(y^2 - 1) = 2B/\hat{\lambda}$. For real

magnets k_0 must be taken somewhat below the inverse lattice distance, so that effective rotation and translation symmetries apply. Correspondingly, χ and H are the effective normalized spin field and the effective Hamiltonian at this scale. Our choice of potential encompasses a large class of field-theoretical and statistical systems. In a different context our results can also be applied to the problem of quantum tunnelling in a (2+1)-dimensional theory at zero temperature. In this case k_0, m^2, γ and λ bare no relation to temperature.

We compute the form of the potential U_k at scales $k \leq k_0$ by integrating an evolution equation [8]. The latter is derived from an exact flow equation for Γ_k [7], typical of the Wilson approach to the renormalization group [9]. The form of U_k changes as the effect of fluctuations with momenta above the decreasing scale k is incorporated in the effective couplings of the theory. We consider an arbitrary form of U_k which, in general, is not convex for non-zero k . U_k approaches the convex effective potential only in the limit $k \rightarrow 0$. In the region relevant for a first-order phase transition, U_k has two distinct local minima. The nucleation rate should be computed for k larger than or around the scale k_f at which U_k starts receiving important contributions from field configurations that interpolate between the two minima. This happens when the negative curvature at the top of the barrier becomes approximately equal to $-k^2$ [10]. Another consistency check for the above choice of k is provided by the fact that for $k > k_f$ the typical length scale of a thick-wall critical bubble is $\gtrsim 1/k$.

We use here a mass-like infrared cutoff k for the fluctuations that are incorporated in Γ_k and neglect the anomalous dimension. The evolution equation for the potential is [7, 8, 6]

$$\begin{aligned} \frac{\partial}{\partial k^2} [U_k(\phi) - U_k(0)] = \\ = -\frac{1}{8\pi} \left[\sqrt{k^2 + U_k''(\phi)} - \sqrt{k^2 + U_k''(0)} \right]. \end{aligned} \quad (3)$$

It is instructive to compare with the first step of an iterative solution of the general flow equation [11]

$$\begin{aligned} U_k^{(1)}(\phi) - U_k^{(1)}(0) = U_{k_0}(\phi) - U_{k_0}(0) + \\ + \frac{1}{2} \ln \left[\frac{\det[-\partial^2 + k^2 + U_k''(\phi)] \det[-\partial^2 + k_0^2 + U_k''(0)]}{\det[-\partial^2 + k_0^2 + U_k''(\phi)] \det[-\partial^2 + k^2 + U_k''(0)]} \right]. \end{aligned} \quad (4)$$

For $k \rightarrow 0$ this is a regularized one-loop approximation to the effective potential. Due to the ratio of determinants, only momentum modes with $k^2 < q^2 < k_0^2$ are effectively included in the momentum integrals in (4). (Eq. (3) can be derived formally from eq. (4) by performing the momentum integration, i.e. $\ln \det F(q^2) = \int \ln F(q^2) d^3q/(2\pi)^3$, and

taking the derivative $\partial/\partial k^2$ assuming that it does not act on U_k).

The nucleation rate per unit volume I (probability of nucleation of a critical bubble per unit time and volume) is $I = A_k \exp(-S_k)$, where $S_k = \int d^3r [-\frac{1}{2}\phi_b(r)\Delta\phi_b(r) + U_k(\phi_b(r))]$ is evaluated for the bubble solution $\phi_b(r)$ which is a saddle point of S_k and interpolates between the true and the false vacuum. The pre-exponential factor is

$$A_k = \frac{E_0}{2\pi} \left(\frac{S_k}{2\pi}\right)^{3/2} \left[\frac{\det' [-\partial^2 + U_k''(\phi_b(r))]}{\det [-\partial^2 + k^2 + U_k''(\phi_b(r))]} \times \frac{\det [-\partial^2 + k^2 + U_k''(0)]}{\det [-\partial^2 + U_k''(0)]} \right]^{-1/2}. \quad (5)$$

Eq. (5) is the standard expression for the nucleation rate [2, 4] with fluctuation determinants replaced by ratios of determinants, in complete analogy to eq. (4). This ensures that only fluctuations with momenta $q^2 \lesssim k^2$ are included in A_k . One observes that, up to the difference between the saddle point $\phi_b(r)$ and the constant field ϕ , the explicit k -dependence of $-\ln I$ cancels between the one-loop contribution to U_k (see eq. (4)) and $-\ln A_k$. The prime in the fluctuation determinant around the saddle point denotes that the three zero eigenvalues are not included. Their contribution generates the factor $(S_k/2\pi)^{3/2}$ and the volume factor that is absorbed in the definition of I . The quantity E_0 is the square root of the absolute value of the unique negative eigenvalue. This last contribution appears only for the high-temperature field theory [4]. It is absent in the expression for the quantum-tunnelling rate in the zero-temperature (2+1)-dimensional theory.

The coarse-grained potential U_k is determined through the numerical integration of eq. (3) between the scales k_0 and k , using, for example, algorithms from ref. [12]. The initial condition for the integration is given by eq. (1). The computation of S_k and A_k is presented in detail in ref. [6], where techniques from refs. [13] are adopted. In contrast to refs. [13], our calculation is ultraviolet finite and no additional regularization is needed.

A possible k -dependence of the final result for the nucleation rate may result from three sources: The first is an insufficiency of the one-loop approximation for $\ln A_k$ which may not match with the more precise non-perturbative determination of S_k . This error grows with increasing k . The second error comes from the replacement of $\phi_b(r)$ by a slowly varying field in the computation of U_k and S_k . It increases with decreasing k and may become substantial for $k < k_f$. Finally, the critical bubble $\phi_b(r)$ is determined by an extremization procedure which does not take into account the contributions to the free energy from fluctuations with momenta smaller than k . It is certainly a

necessary requirement for the validity of Langer's nucleation theory that the k -dependence of the nucleation rate comes out small in some appropriate range of k [14] (typically near k_f). Furthermore, nucleation theory will break down if the rate ceases to be exponentially suppressed. This typically happens near the spinodal line (along which the false vacuum becomes unstable), and, in particular, in the vicinity of the endpoint of the first-order critical line — in our case at a second-order phase transition. For the potential of eq. (1), the two first-order critical lines obey $\gamma_{k_0}^2 = 9\lambda_{k_0}m_{k_0}^2$ and $\gamma_{k_0} = 0$, with endpoints at $m_{k_0}^2 = -2\mu_{\text{cr}}^2$, $\gamma_{k_0}^2 = -18\lambda_{k_0}\mu_{\text{cr}}^2$ and $m_{k_0}^2 = \mu_{\text{cr}}^2$, $\gamma_{k_0} = 0$ [15]. Here μ_{cr}^2 is the critical mass term of the Ising model ($\mu_{\text{cr}}^2/k_0^2 \approx -0.0115$ for $\lambda_{k_0}/k_0 = 0.1$). We point out that, for fixed $m_{k_0}^2$ and λ_{k_0} , opposite values of γ_{k_0} result in potentials related through $\phi \leftrightarrow -\phi$. Also a model with $m_{k_0}^2 < 0$ can be mapped onto the equivalent model with $m_{k_0}^2 > 0$ by the shift $\phi \rightarrow \phi + c$, $\lambda_{k_0}c^2 + \gamma_{k_0}c = -2m_{k_0}^2$, where $m_{k_0}^2 = -2m_{k_0}^2 - \frac{1}{2}\gamma_{k_0}c$, $\gamma'_{k_0} = \gamma_{k_0} + 3\lambda_{k_0}c$.

3. Sample computations: We present here a computation of the spontaneous nucleation rate and establish the region of validity of Langer's theory. Fig. 1 exhibits the results of our calculation for the potential (1) with $m_{k_0}^2 = -0.0433 k_0^2$, $\gamma_{k_0} = -0.0634 k_0^{3/2}$, $\lambda_{k_0} = 0.1 k_0$. We first show in fig. 1a the evolution of the potential $U_k(\phi)$ as the scale k is lowered. (We always shift the metastable vacuum to $\phi = 0$.) The solid line corresponds to $k/k_0 = 0.513$ while the line with longest dashes (that has the smallest barrier height) corresponds to $k_f/k_0 = 0.223$. At the scale k_f the negative curvature at the top of the barrier is slightly larger than $-k_f^2$ and we stop the evolution. The potential and the field have been normalized with respect to k_f . As k is lowered from k_0 to k_f , the absolute minimum of the potential settles at a non-zero value of ϕ , while a significant barrier separates it from the metastable minimum at $\phi = 0$. The profile of the critical bubble $\phi_b(r)$ is plotted in fig. 1b in units of k_f for the same sequence of scales. For $k \simeq k_f$ the characteristic length scale of the bubble profile and $1/k$ are comparable. This is expected, because the form of the profile is determined by the barrier of the potential, whose curvature is $\simeq -k^2$ at this point. This is an indication that we should not proceed to coarse-graining scales below k_f . We observe a significant variation of the value of the field ϕ in the interior of the bubble for different k .

Our results for the nucleation rate are presented in fig. 1c. The horizontal axis corresponds to $k/\sqrt{U_k''(\phi_t)}$, i.e. the ratio of the scale k to the square root of the positive curvature (equal to the mass of the field) at the absolute minimum of the potential located at ϕ_t . Typically, when k

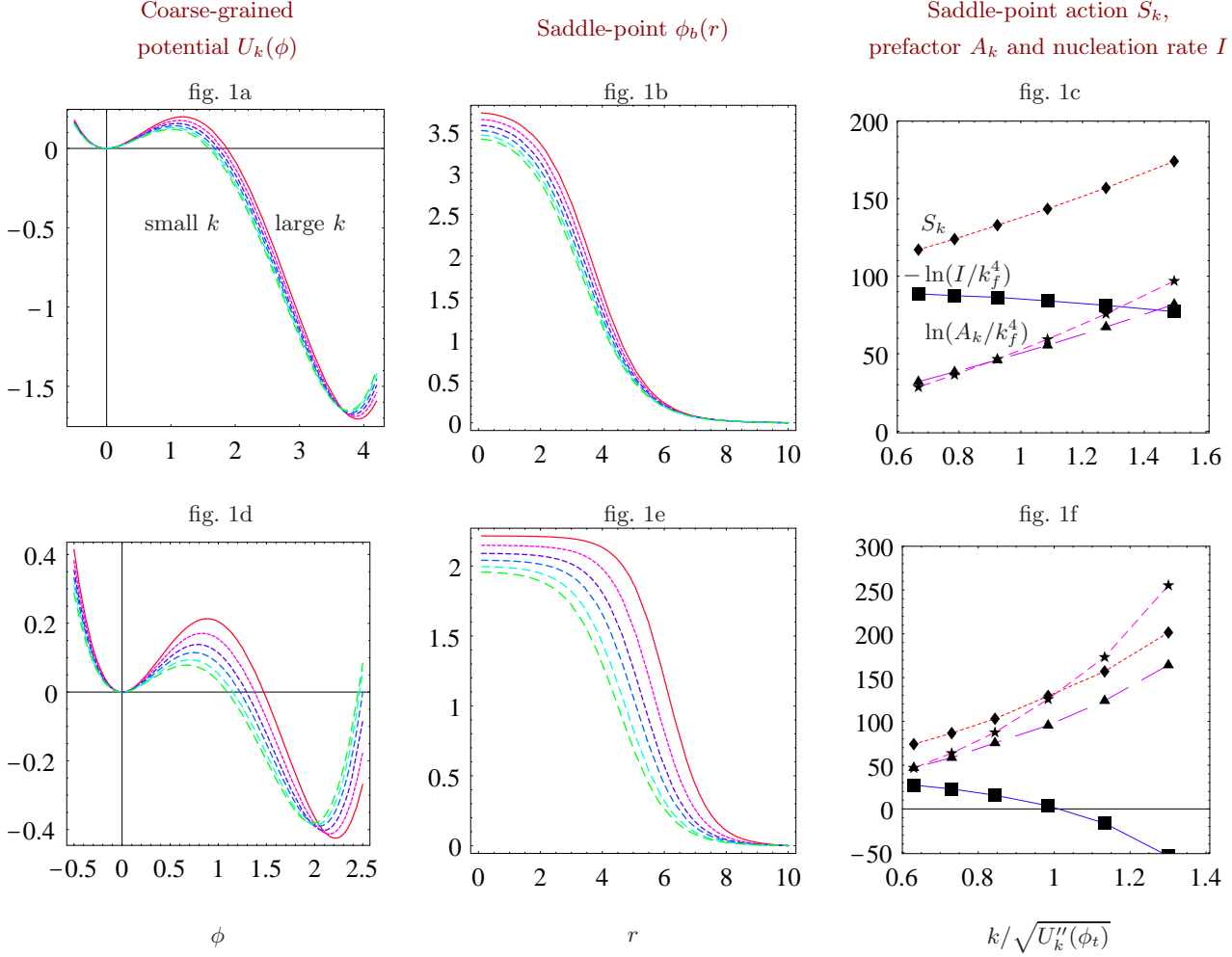


Figure 1: *Dependence of effective potential, critical bubble and nucleation rate on the coarse graining scale k . The parameters are $\lambda_{k_0} = 0.1 \cdot k_0$, $m_{k_0}^2 = -0.0433 \cdot k_0^2$, $\gamma_{k_0} = -0.0634 \cdot k_0^{3/2}$ (figs. 1a–1c) and $m_{k_0}^2 = -0.013 \cdot k_0^2$, $\gamma_{k_0} = -1.61 \cdot 10^{-3} \cdot k_0^{3/2}$ (figs. 1d–1f). All dimensional quantities are given in units of k_f , equal to $0.223 \cdot k_0$ in the first series and to $0.0421 \cdot k_0$ in the second series.*

crosses below this mass, the massive fluctuations of the field start decoupling. The evolution of the convex parts of the potential slows down and eventually stops. The dark diamonds give the values of the action S_k (free energy rescaled by the temperature) of the critical bubble at the scale k . We observe a strong k dependence of this quantity, which is expected from the behaviour in figs. 1a, 1b. The stars in fig. 1c indicate the values of $\ln(A_k/k_f^4)$. Again a substantial decrease with decreasing k is observed. This is expected, because k acts as the effective ultraviolet cutoff in the calculation of the fluctuation determinants in A_k . The dark squares give our results for $-\ln(I/k_f^4) = S_k - \ln(A_k/k_f^4)$. It is remarkable that the k dependence of this quantity almost

disappears for $k/\sqrt{U''_k(\phi_t)} \lesssim 1$. The small residual dependence on k can be used to estimate the contribution of the next order in the expansion around the saddle point. It is reassuring that this contribution is expected to be smaller than $\ln(A_k/k_f^4)$.

This behaviour confirms our expectation that the nucleation rate should be independent of the scale k that we introduced as a calculational tool. It also demonstrates that all the configurations plotted in fig. 1b give equivalent descriptions of the system, at least for the lower values of k . This indicates that the critical bubble should not be associated only with the saddle point of the semiclassical approximation, whose action is scale dependent. It is the

combination of the saddle point and its possible deformations in the thermal bath that has physical meaning. We point out that a reliable calculation of the nucleation rate is only possible if the ultraviolet cutoff in the fluctuation determinant matches properly with the infrared scale in the coarse-graining procedure. This problem was not quantitatively accessible before the present work.

For smaller values of $|m_{k_0}^2|$ the dependence of the nucleation rate on k becomes more pronounced. We demonstrate this in the second series of figs. 1d–1f where $(-m_{k_0}^2)^{1/2}/\lambda_{k_0} = 1.13$ (instead of 2.08 for figs. 1a–1c). The value of λ_{k_0} is the same as before, whereas $\gamma_{k_0} = -1.61 \cdot 10^{-3} k_0^{3/2}$ and $k_f/k_0 = 0.0421$. The reason for this behaviour is the larger value of the dimensionless renormalized quartic coupling [14] for the second parameter set. Higher loop contributions to A_k become more important.

It is apparent from figs. 1c and 1f that the leading contribution to the pre-exponential factor increases the total nucleation rate. This behaviour, related to the fluctuations of the field whose expectation value serves as the order parameter, is observed in multi-field models as well. The reason can be traced to the form of the differential operators in the prefactor of eq. (5). This prefactor involves the ratio $\det'[-\partial^2 + U_k''(\phi_b(r))]/\det[-\partial^2 + U_k''(0)]$ before regularization. The function $U_k''(\phi_b(r))$ always has a minimum away from $r = 0$ where it takes negative values (corresponding to the negative curvature at the top of the barrier), while $U_k''(0)$ is always positive. As a result the lowest eigenvalues of the operator $\det'[-\partial^2 + U_k''(\phi_b(r))]$ are smaller than those of $\det[-\partial^2 + U_k''(0)]$. The elimination of the very large eigenvalues from the determinants through regularization does not affect this fact and the prefactor is always larger than 1. Moreover, for weak first-order phase transitions it becomes exponentially large because of the proliferation of low eigenvalues of the first operator. In physical terms, this implies the existence of a large class of field configurations of free energy comparable to that of the saddle-point. Despite the fact that they are not saddle points of the free energy (they are rather deformations of a saddle point) and are, therefore, unstable, they result in a dramatic increase of the nucleation rate. This picture is very similar to that of “subcritical bubbles” of ref. [16].

4. Approximate expression for the prefactor:

In figs. 1c and 1f we also display the values of $\ln(A_k/k_f^4)$ (dark triangles) predicted by the approximate expression

$$\ln \frac{A_k}{k_f^4} \approx \frac{\pi k}{2} \left[- \int_0^\infty r^3 [U_k''(\phi_b(r)) - U_k''(0)] dr \right]^{1/2} \equiv D\pi. \quad (6)$$

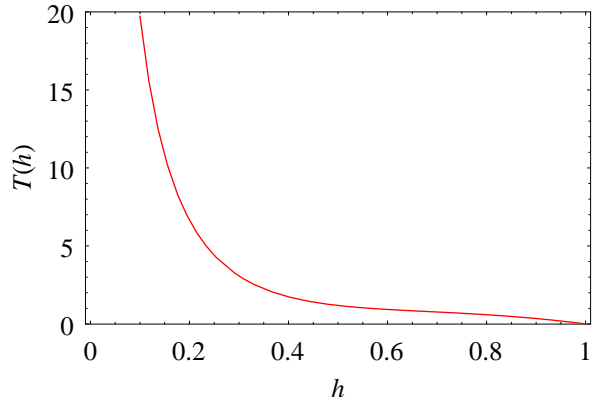


Figure 2: The parameter $T(h)$, defined in eq. (11), as a function of h .

This expression is obtained as follows: The prefactor, given by a combination of determinants involving the Laplacian operator, can be written as a product of contributions with fixed angular momentum number ℓ : $A_k = \prod_\ell c_\ell$. For large ℓ , the factors c_ℓ can be evaluated analytically as $c_\ell = 1 + D^2/\ell^2 + \mathcal{O}(\ell^{-4})$ [6]. We have checked that the first two terms of this expansion give a good approximation to c_ℓ even for $\ell \lesssim D$, except for $\ell = \mathcal{O}(1)$. Unless the prefactor is of order 1, we obtain $A_k \approx \prod_\ell c_\ell \approx e^{D\pi}$.

Eq. (6) permits a quick evaluation of the prefactor in terms of the bubble profile. It is useful to obtain some intuition on the behaviour of the nucleation rate by using this expression. We assume that the potential has an approximate form similar to eq. (1) even near k_f , i.e.

$$U_{k_f}(\phi) \approx \frac{1}{2} m_{k_f}^2 \phi^2 + \frac{1}{6} \gamma_{k_f} \phi^3 + \frac{1}{8} \lambda_{k_f} \phi^4, \quad (7)$$

with $m_{k_f}^2 > 0$. For systems not very close to the endpoint of the first-order critical line, this assumption is supported by the numerical data, as can be verified from fig. 1. The scale k_f is determined by the relation

$$k_f^2 \approx \max |U_{k_f}''(\phi)| = \frac{\gamma_{k_f}^2}{6\lambda_{k_f}} - m_{k_f}^2. \quad (8)$$

Through the rescalings $r = \tilde{r}/m_{k_f}$, $\phi = 2\tilde{\phi} m_{k_f}^2/\gamma_{k_f}$, the potential can be written as

$$\tilde{U}(\tilde{\phi}) = \frac{1}{2} \tilde{\phi}^2 - \frac{1}{3} \tilde{\phi}^3 + \frac{h}{18} \tilde{\phi}^4,$$

with $h = 9\lambda_{k_f} m_{k_f}^2/\gamma_{k_f}^2$. For $h \approx 1$ the two minima of the potential have approximately equal depth. The action of the saddle point can be expressed as

$$S_{k_f} = \frac{4}{9} \frac{m_{k_f}}{\lambda_{k_f}} h \tilde{S}(h), \quad (9)$$

where $\tilde{S}(h)$ must be determined numerically through $\tilde{U}(\tilde{\phi})$. Similarly, the pre-exponential factor can be estimated through eq. (6) as

$$\begin{aligned} \ln \frac{A_{k_f}}{k_f^4} &\approx \frac{\pi}{2} \sqrt{\frac{3}{2h} - 1} \tilde{A}(h), \\ \tilde{A}^2(h) &= \int_0^\infty \tilde{U}''(\tilde{\phi}_b(\tilde{r})) \tilde{r}^3 d\tilde{r}, \end{aligned} \quad (10)$$

with $\tilde{A}(h)$ computed numerically. Finally

$$R = \frac{\ln(A_{k_f}/k_f^4)}{S_{k_f}} \approx \frac{9\pi}{8h} \sqrt{\frac{3}{2h} - 1} \frac{\tilde{A}(h)}{\tilde{S}(h)} \frac{\lambda_{k_f}}{m_{k_f}} = T(h) \frac{\lambda_{k_f}}{m_{k_f}}. \quad (11)$$

In fig. 2 we plot $T(h)$ as a function of h in the interval $(0, 1)$. It diverges for $h \rightarrow 0$. For $h \rightarrow 1$, our estimate of the prefactor predicts $T(h) \rightarrow 0$. The reason is that, for our approximate potential of eq. (7), the field masses at the two minima are equal in this limit. As a result, the integrand in eq. (6) vanishes, apart from at the surface of the bubble. The small surface contribution is negligible for $h \rightarrow 1$, because the critical bubbles are very large in this limit. This behaviour is not expected to persist for more complicated potentials. Instead, we expect a constant value of $T(h)$ for $h \rightarrow 1$. However, the approximate expression (6) has not been tested for very large critical bubbles. The divergence of the saddle-point action in this limit results in low accuracy for our numerical analysis. Typically, our results are reliable for $\tilde{S}(h)$ less than a few thousand. Also, eq. (6) relies on a large- ℓ approximation. For increasing D , this breaks down below an increasing value ℓ_{as} and, therefore, eq. (6) is not guaranteed to be valid. We have checked that both our numerical and approximate results are reliable for $h \lesssim 0.9$.

The estimate of eq. (11) suggests two cases in which the expansion around the saddle point is expected to break down:

- a) For fixed λ_{k_f}/m_{k_f} , the ratio R becomes larger than 1 for $h \rightarrow 0$. In this limit the barrier becomes negligible and the system is close to the spinodal line.
- b) For fixed h , again R can be large for sufficiently large λ_{k_f}/m_{k_f} .

Case (b) is possible even for h close to 1, so that the system is far from the spinodal line. This case corresponds to weak first-order phase transitions, as can be verified by observing that the saddle-point action of eq. (9), the location of the true vacuum

$$\frac{\phi_t}{\sqrt{m_{k_f}}} = \frac{2}{3} \sqrt{h} \tilde{\phi}_t(h) \sqrt{\frac{m_{k_f}}{\lambda_{k_f}}}, \quad (12)$$

and the difference in free-energy density between the min-

$$\frac{\Delta U}{m_{k_f}^3} = \frac{4}{9} h \Delta \tilde{U}(h) \frac{m_{k_f}}{\lambda_{k_f}} \quad (13)$$

go to zero in the limit $m_{k_f}/\lambda_{k_f} \rightarrow 0$ for fixed h . This is in agreement with the discussion of fig. 1 in the previous section.

The breakdown of homogeneous nucleation theory in both the above cases is confirmed through the numerical computation of the nucleation rates.

5. The region of validity of homogeneous nucleation theory:

In fig. 3 we show contour plots for I/k_f^4 and for $R = \ln(A_{k_f}/k_f^4)/S_{k_f}$ in the $(m_{k_0}^2, \gamma_{k_0})$ plane for fixed $\lambda_{k_0}/k_0 = 0.1$. One can see the decrease of the rate as the first-order critical line $\gamma_{k_0} = 0$ is approached. The spinodal line (end of the shaded region), on which the metastable minimum of U_k becomes unstable, is also shown. The nucleation rate becomes large before the spinodal line is reached. For $-\ln(I/k_f^4)$ of order 1, the exponential suppression of the nucleation rate disappears. Langer's approach can no longer be applied and an alternative picture for the dynamical transition must be developed [17]. In the region between the contour $I/k_f^4 = e^{-3}$ and the spinodal line, one expects a smooth transition from nucleation to spinodal decomposition. The spinodal and critical lines meet at the endpoint in the lower right corner, which corresponds to a second order phase transition. The figure exhibits an increasing rate as the endpoint is approached at a fixed distance from the critical line.

The ratio R is a measure of the validity of the semiclassical approximation. For $R \approx 1$ the fluctuation determinant is as important as the "classical" exponential factor e^{-S_k} . There is no reason to assume that higher loop contributions from the fluctuations around the critical bubble can be neglected anymore. Near the endpoint in the lower right corner, Langer's semiclassical picture breaks down, despite the presence of a discontinuity in the order parameter. Requiring $I/k_f^4 \lesssim e^{-3}$, $R \lesssim 1$, gives a limit of validity for Langer's theory. For a fixed value of the nucleation rate (solid lines in fig. 3), the ratio R grows as the endpoint in the lower right corner is approached. This indicates that Langer's theory is not applicable for weak first-order phase transitions, even if the predicted rate is exponentially suppressed. The concept of nucleation of a region of the stable phase within the metastable phase may still be relevant. However, a quantitative estimate of the nucleation rate requires taking into account fluctuations of the system that are not described properly by the semiclassical approximation [16].

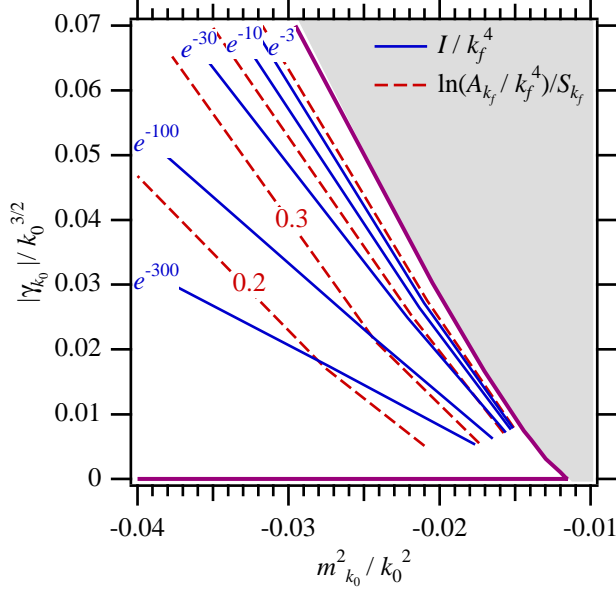


Figure 3: Contour plots of I/k_f^4 and of $R = \ln(A_{k_f}/k_f^4)/S_{k_f}$ in the plane $(m_{k_0}^2, \gamma_{k_0})$, for $\lambda_{k_0}/k_0 = 0.1$. Regions to the right of the spinodal line (only one minimum) are shaded. The dashed lines correspond to $R = \{0.2, 0.3, 0.5, 1\}$ and the solid lines to I/k_f^4 .

The parameter region discussed here may be somewhat unusual since the critical line of the phase transition is approached by varying γ_{k_0} from negative or positive values towards zero. We have chosen it only for making the graph more transparent. However, the results of fig. 3 can be mapped by a shift $\phi \rightarrow \phi + c$ to another region with $m_{k_0}^2 > 0$, for which the first-order phase transition can be approached by varying $m_{k_0}^2$ at fixed γ_{k_0} (see end of section 2). As opposite values of γ_{k_0} result in potentials related by $\phi \leftrightarrow -\phi$, we can always choose $\gamma_{k_0} < 0$. Then the phase transition proceeds from a metastable minimum at the origin to a stable minimum along the positive ϕ -axis (as in fig. 1a). Potentials with $m_{k_0}^2 > 0$, $\gamma_{k_0} < 0$ are relevant for cosmological phase transitions, such as the electroweak.

In fig. 4 we depict the region of validity of homogeneous nucleation theory in terms of parameters of the low-energy theory at the scale k_f . The contours correspond to the same quantities as in fig. 3, which are now plotted as a function of the renormalized mass at the false vacuum $m_f = U_{k_f}''(0)^{1/2}$ in units of k_0 and the difference in free-energy density between the two vacua in units of m_f^3 . Here m_f^{-1} corresponds to the correlation length in the false vacuum and $\Delta U/m_{k_f}^3$ can be related to observable quantities like the jump in the order parameter or the latent heat if λ_{k_0}/k_0 is kept fixed.

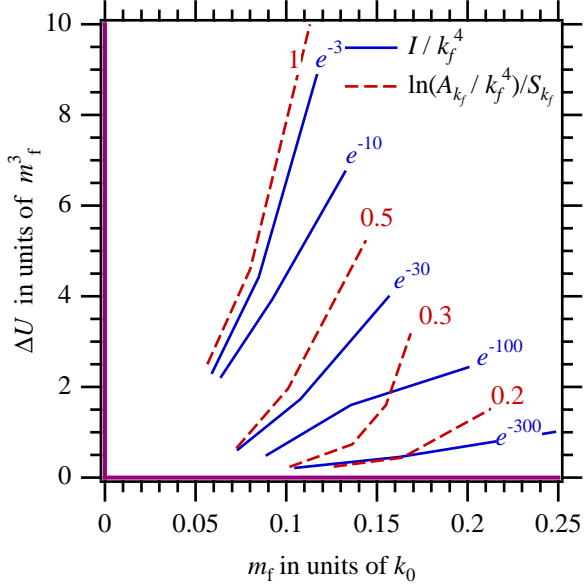


Figure 4: The contour plots of fig. 3 in the plane $(m_f, \Delta U)$, where m_f is the mass at the false vacuum and ΔU is the difference in free-energy density between the two vacua. The spinodal line corresponds to the vertical axis.

(Similarly, for given λ_{k_f}/m_{k_f} , we can relate $\Delta U/m_{k_f}^3$ to h in the approximation of eq. (7) using eq. (13)). The spinodal line corresponds to the vertical axis, as for $m_f = 0$ the origin of the potential turns into a maximum. The critical line corresponds to the horizontal axis. The origin is the endpoint of the critical line. During the evolution between the scales k_0 and k_f , the quartic coupling becomes larger than its initial value $\lambda_{k_0}/k_0 = 0.1$. All the potentials we have studied have an approximate form similar to eq. (7) with $h \lesssim 0.9$. From our discussion in the previous section and fig. 2 we expect that R is approximately given by eq. (6) with $T(h) \gtrsim 0.3$ for $h \lesssim 0.9$. This indicates that $R \gtrsim 1$ for $m_f/k_0 \lesssim 0.05$ even far from the spinodal line. This expectation is confirmed by fig. 4. Even for theories with a significant exponential suppression for the estimated nucleation rate we expect $R \sim 1$ near $m_f/k_0 \approx 0.05$.

6. Final comments: In the above discussion we have normalized the dimensionful quantities such as I and A_k with respect to k_f , which is the natural scale associated with tunnelling. In the context of thermal field theories, the nucleation rate is often expressed in units of the temperature, which may be identified with the scale k_0 in our approach. As k_f can be substantially lower than k_0 , the

breakdown of the semiclassical approximation (signalled by $R \sim 1$) can occur for values of I/k_0^4 much smaller than those of I/k_f^4 .

For a dynamical process with temperature slowly varying on a characteristic time scale t_{ch} , the phase transition will essentially take place for $I/k_f^3 = t_{\text{ch}}^{-1}$. For a known temperature dependence of the parameters in eq. (1) within the region of validity of Langer's theory, our results permit a precise prediction of the amount of supercooling by extracting from fig. 3 the effective transition temperature. An approximate value of this temperature can also be obtained by determining the bubble profile numerically and using eq. (6) in order to estimate the pre-exponential factor.

Finally, we point out that realistic statistical systems often have large dimensionless couplings $\lambda_{k_0}/k_0 \sim 10$. Our results indicate that Langer's homogeneous nucleation theory breaks down for such systems even for small correlation lengths in the metastable phase ($m_f/k_0 \sim 1$). Furthermore, for a large enough correlation length the first-order phase transition displays universal behaviour with large $\lambda_{k_f}/m_f \approx 5$, independently of the short-distance couplings [8, 15]. We conclude that a saddle-point approximation for the fluctuations around the critical bubble does not give accurate results in the universal region.

Acknowledgements: The work of N.T. and C.W. is supported by the E.C. under TMR contract Nos. ERBF-MRX-CT96-0090 and ERBF-MRX-CT97-0122.

References

- [1] P.A. Rikvold and B.M. Gorman, Ann. Rev. Comput. Phys. I, edited by D. Stauffer, (World Scientific, Singapore, 1994) p. 149.
- [2] J. Langer, Ann. Phys. **41**, 108 (1967); *ibid.* **54**, 258 (1969); Physica **73**, 61 (1974).
- [3] S. Coleman, Phys. Rev. D, **15**, 2929 (1977); C.G. Callan and S. Coleman, Phys. Rev. D, **16**, 1762 (1977).
- [4] I. Affleck, Phys. Rev. Lett. **46**, 388 (1981); A.D. Linde, Nucl. Phys. B **216**, 421 (1983).
- [5] L.P. Csernai and J.I. Kapusta, Phys. Rev. D **46**, 1379 (1992).
- [6] A. Strumia and N. Tetradis, Nucl. Phys. B **542**, 719 (1999).
- [7] C. Wetterich, Phys. Lett. B **301**, 90 (1993); Nucl. Phys. B **352**, 529 (1991); Z. Phys. C **57**, 451 (1993); *ibid.* **60**, 461 (1993).
- [8] N. Tetradis and C. Wetterich, Nucl. Phys. B **398**, 659 (1993); B **422**, 541 (1994); Int. J. Mod. Phys. A **9**, 4029 (1994); N. Tetradis, Nucl. Phys. B **488**, 92 (1997); J. Berges, N. Tetradis and C. Wetterich, Phys. Rev. Lett. **77**, 873 (1996).
- [9] K.G. Wilson and I.G. Kogut, Phys. Rep. **12**, 75 (1974); F.J. Wegner and A. Houghton, Phys. Rev. A **8**, 401 (1973); S. Weinberg, Critical phenomena for field theorists, in Erice Subnuc. Phys. 1 (1976); J. Polchinski, Nucl. Phys. B **231**, 269 (1984).
- [10] A. Ringwald and C. Wetterich, Nucl. Phys. B **334**, 506 (1990); N. Tetradis and C. Wetterich, Nucl. Phys. B **383**, 197 (1992).
- [11] C. Wetterich, Mod. Phys. Lett. **A11** (1996) 2573.
- [12] J. Adams, J. Berges, S. Bornholdt, F. Freire, N. Tetradis and C. Wetterich, Mod. Phys. Lett. A **10**, 2367 (1995).
- [13] W.N. Cottingham, D. Kalafatis and R. Vinh Mau, Phys. Rev. B **48**, 6788 (1993); J. Baacke and V.G. Kiselev, Phys. Rev. D **48**, 5648 (1993); J. Baacke, *ibid.* **52**, 6760 (1995).
- [14] J. Berges, N. Tetradis and C. Wetterich, Phys. Lett. B **393**, 387 (1997); J. Berges and C. Wetterich, Nucl. Phys. B **487**, 675 (1997).
- [15] S. Seide and C. Wetterich, preprint HD-THEP-98-20, cond-mat/9806372.
- [16] M. Gleiser, E.W. Kolb and R. Watkins, Nucl. Phys. B **364**, 411 (1991); M. Gleiser and E.W. Kolb, Phys. Rev. Lett. **69**, 1304 (1992); Phys. Rev. D **48**, 1560 (1993); N. Tetradis, Z. Phys. C **57**, 331 (1993); G. Gelmini and M. Gleiser, Nucl. Phys. B **419**, 129 (1994); M. Gleiser, Phys. Rev. Lett. **73**, 3495 (1994); Phys. Rev. D **49**, 2978 (1994); E.J. Copeland, M. Gleiser and H.-R. Müller, Phys. Rev. D **52**, 1920 (1995); M. Gleiser, A. Heckler and E.W. Kolb, Phys. Lett. B **405**, 121 (1997); J. Borrill and M. Gleiser, Nucl. Phys. B **483**, 416 (1997).
- [17] D. Boyanovsky, H.J. de Vega, R. Holman, D.S. Lee and A. Singh, Phys. Rev. D **51**, 4419 (1995); D. Boyanovsky, M. D'Attanasio, H.J. de Vega, R. Holman and D.S. Lee, Phys. Rev. D **52**, 6805 (1995); F. Cooper, S. Habib, Y. Kluger and E. Mottola, Phys. Rev. D **55**, 6471 (1997); D. Boyanovsky, H.J. de Vega, R. Holman, S. Prem Kumar and R.D. Pisarski, Phys. Rev. D **57**, 3653 (1998); D. Boyanovsky, H.J. de Vega, R. Holman and J. Salgado, preprint LP-THE-98-45 and hep-ph/9811273.